SUPPORTING INFORMATION

Salt bridge dynamics in protein/DNA recognition: a comparative analysis of Elk1 and ETV6

May 22, 2021

Tam D. Vo,[1,*] Amelia L. Schneider,[1] W. David Wilson[1,2,**] and Gregory M. K. Poon[1,2,**]

[1] Department of Chemistry

[2] Center for Diagnostics and Therapeutics

Georgia State University

Atlanta, GA 30303

* Current address: National Cancer Institute, National Institutes of Health, Bethesda, MD 20892

** To whom correspondence should be addressed P.O. Box 3965, Atlanta, GA 30302-3965. Email: gpoon@gsu.edu and wdw@gsu.edu. Tel. (404) 413-5491 and (404) 413-5498.

INDEX TO SUPPLEMENT

SUPPLEMENTAL TABLES

Table S1. Biosensor-SPR steady-state analysis of Elk1 binding to E74 and SC1.

$[Na^+]$, M	K_D, $\times 10^{-9}$ M	
	E74	**SC1**
0.2	0.1 ± 0.2	0.3 ± 0.1
0.25	0.4 ± 0.1	1.4 ± 0.05
0.3	1.0 ± 0.1	3.8 ± 0.08
0.35	2.6 ± 0.2	10.6 ± 0.4
0.4	6.3 ± 0.2	22.7 ± 0.3
0.5	30.9 ± 0.4	108 ± 1.4
0.6	72.1 ± 1.4	281 ± 5.7
$\Delta m_{obs} = -\frac{\partial \log K_D}{\partial \log[Na^+]}$	-6.0 ± 0.1	-6.0 ± 0.1

Table S2. Nonspecific DNA binding by the ETS domain of Elk1 to salmon sperm DNA.

$[Na^+]$, M	K_D, μM	Cooperativity (ω)
0.15	2.4 ± 0.1	93 ± 10
0.2	7.7 ± 0.8	77 ± 6
0.25	28.3 ± 9.7	62 ± 38
0.3	21.5 ± 6.3	171 ± 14
0.35	69.8 ± 3.2	251 ± 15
0.4	75.8 ± 7.8	601 ± 42
$\Delta m_{ns} = -\frac{\partial \log K_D}{\partial \log[Na^+]}$		-3.1 ± 0.5

Table S3. Electrostatic and phylogenetic characteristics of human ETS domains

ETS domain (residue range)[a]	Index in Fig. 7	# acidic residues	# basic residues	basic / acidic	Isoelectric point	Evolutionary distance
EHF (207-289)	17	11	18	1.64	9.87	0.5556
ELF1 (208-290)	18	7	17	2.43	9.91	0.4938
ELF2 (208-290)	19	8	17	2.13	9.81	0.5062
ELF3 (273-355)	20	11	17	1.55	9.79	0.5556
ELF4 (209-291)	21	7	17	2.43	9.91	0.5062
ELF5 (173-254)	22	13	17	1.31	9.37	0.5750
ELK1 (5-86)	2	8	15	1.88	9.93	0.3827
ELK3 (5-85)	3	8	15	1.88	9.64	0.3750
ELK4 (5-85)	4	4	15	3.75	10.11	0.3875
ERF (27-107)	5	9	17	1.89	9.75	0.4321
ERG (318-398)	6	11	14	1.27	9.07	0.3704
ETS1 (335-415)	7	9	17	1.89	9.79	0.3086
ETS2 (363-443)	8	9	17	1.89	9.79	0.3210
ETV1 (335-415)	9	9	13	1.44	9.52	0.4321
ETV2 (240-320)	10	8	19	2.38	10.28	0.4321
ETV3 (35-116)	11	9	18	2.00	9.90	0.4250
ETV3L (39-120)	12	9	18	2.00	9.90	0.4321
ETV4 (341-421)	13	9	12	1.33	9.30	0.4321
ETV5 (368-448)	14	9	13	1.44	9.52	0.4321
ETV6 (339-420)	23	9	17	1.89	10.13	0.6296
ETV7 (224-305)	24	9	17	1.89	9.88	0.6296
FEV (47-127)	15	11	15	1.36	9.34	0.3704
FLI1 (281-361)	16	11	14	1.27	9.07	0.3704
GABPA (320-400)	1	11	14	1.27	8.93	0.0000
PU.1 (170-253)	25	7	21	3.00	10.32	0.5185
SPEDF (249-332)	28	6	19	3.17	10.55	0.5625
SPIB (169-252)	26	6	20	3.33	10.83	0.5375
SPIC (111-194)	27	7	19	2.71	10.21	0.6250

[a] As curated in the UniProt database (uniprot.org).

SUPPLEMENTAL FIGURES

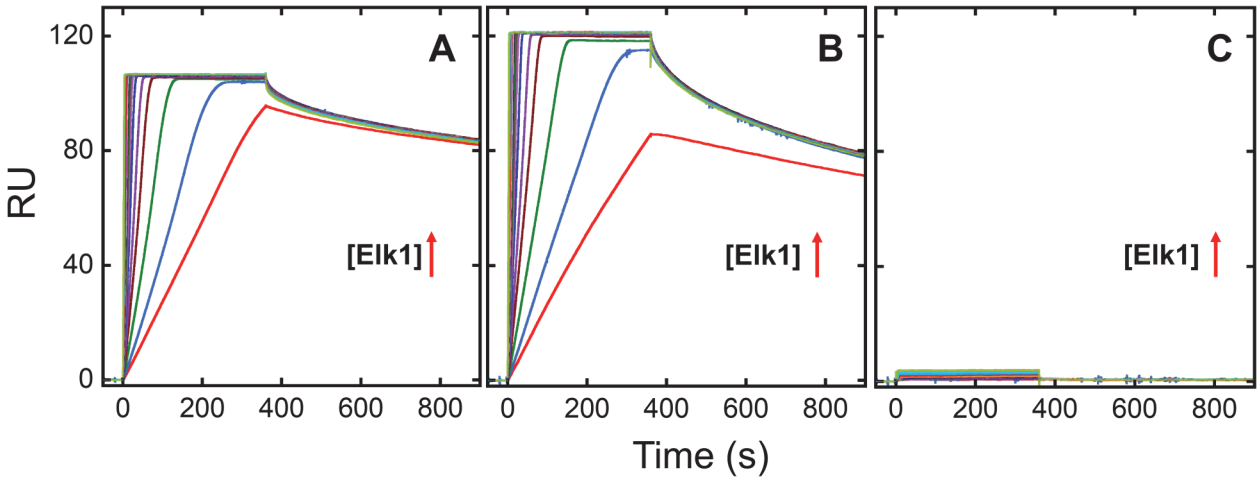

Figure S1. Representative sensorgrams of Elk1 binding to different DNA sequences at 0.15 M Na^+. A, with E74, **B**, with SC1, and **C**, with a nonspecific sequence SD1 (see Materials and Methods). Concentrations of Elk1 were graded from 1 to 150 nM. DNA sequences are immobilized on a streptavidin chip as described in the methods section. Titration with increasing concentration of Elk1 leads to an increase in response units (RU) for DNA sequences containing the 5'-GGAA-3' consensus (E74 and SC1), but negligible binding was observed with a scrambled sequence under identical conditions.

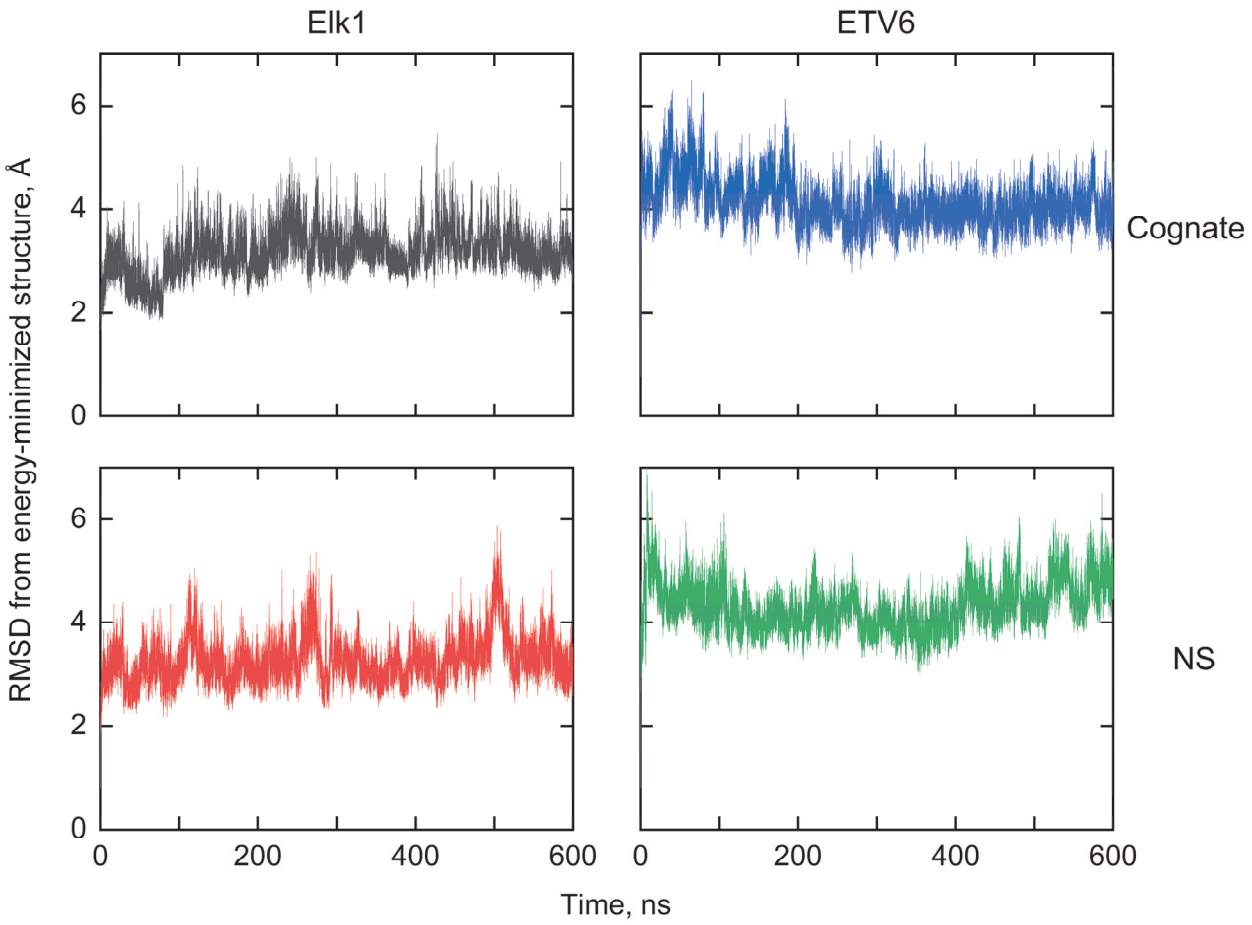

Figure S2. All-atom RMS deviations in MD trajectories of DNA complexes of Elk1 and ETV6. The protein in the respective energy-minimized structures served as reference coordinates for RMSD calculations.

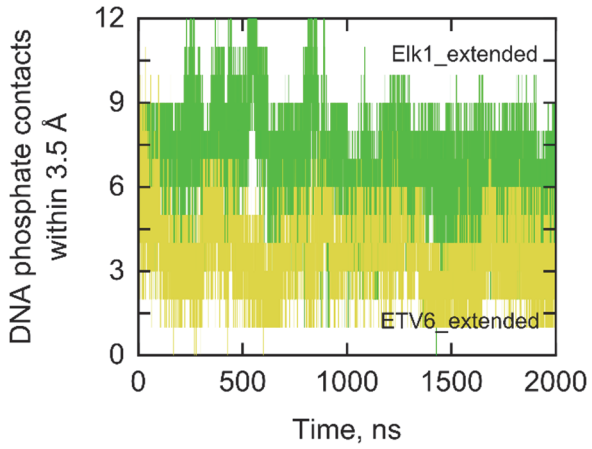

Figure S3. Extended trajectory of DNA phosphate contacts in the nonspecific Elk1 and ETV6 complexes. Illustrative production trajectories of each complex run out to 2 μs. The median ± MAD number of contacts over the final 1 μs of the trajectory is 6 ± 1 for Elk1 and 4 ± 1 for ETV6.

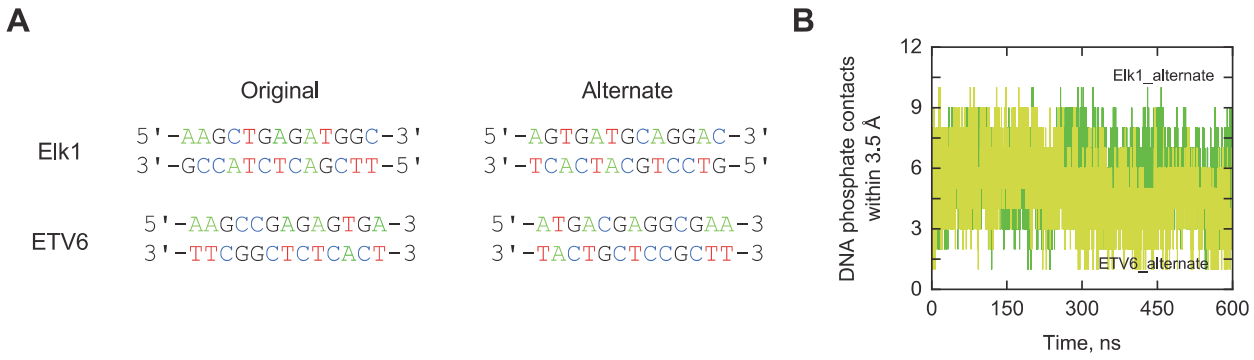

Figure S4. DNA phosphate contacts by alternate nonspecific complexes of Elk1 and ETV6. **A**, Comparison of the nonspecific sequences used in results reported in the main text and a scrambled alternate sequence. **B**, Trajectories of DNA phosphate contacts in the alternate nonspecific complexes. The median ± MAD number of contacts in the final 200 ns of the trajectory is 6 ± 1 for Elk1 and 4 ± 1 for ETV6.

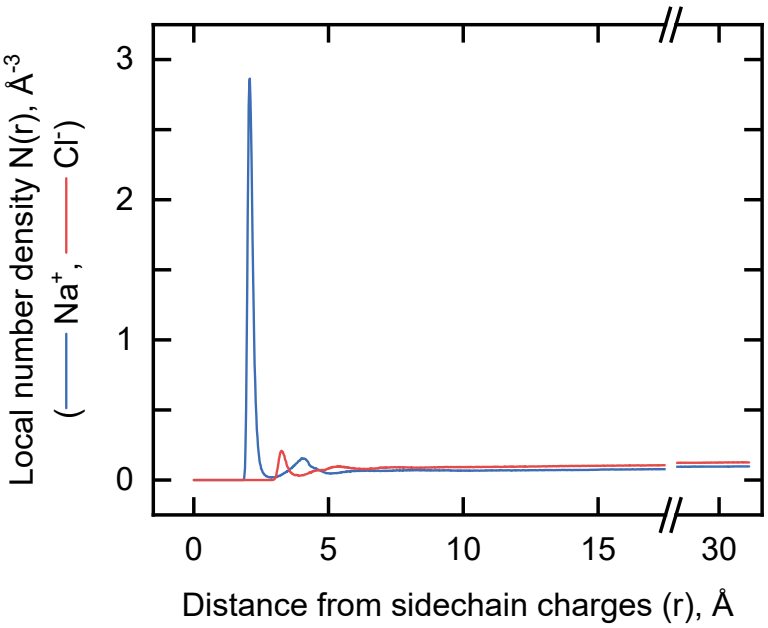

Figure S5. Local ionic densities around charge-bearing atoms in the unbound ETS domain of Elk1. The initial coordinates were templated from the co-crystal structure of the cognate Elk1/DNA complex (1DUX) with the DNA removed, and simulated exactly as for the complexes. Relative to the complexes, the predominance of Na^+ over Cl^- in the primary maxima is maintained, although it is weaker in the absence of polyanionic DNA. Also notable is presence of a peak for Cl^- at r = 3.3 Å, which is absent for the complexes due to strong repulsion by DNA.

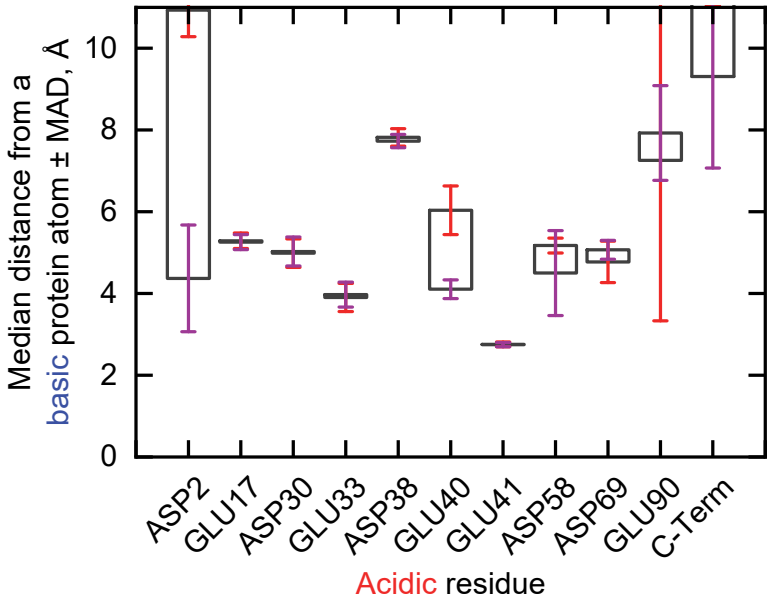

Figure S6. Intramolecular salt bridges in an alternate nonspecifically bound Elk1. As a check on the redistribution of salt bridges in nonspecifically bound Elk1, the alternate Elk1 complex described in Figure S4 is examined. Shown are the median distances of closest approach between cationic atoms from any basic residue to an anionic atom of acidic residues. “Error bars” represent the median absolute deviations (MADs) in the cognate (purple) and nonspecific (red) complex. As in the original nonspecific complex described in the text, Glu40 and Asp2 are the two only acidic residues with non-overlapping MADs.

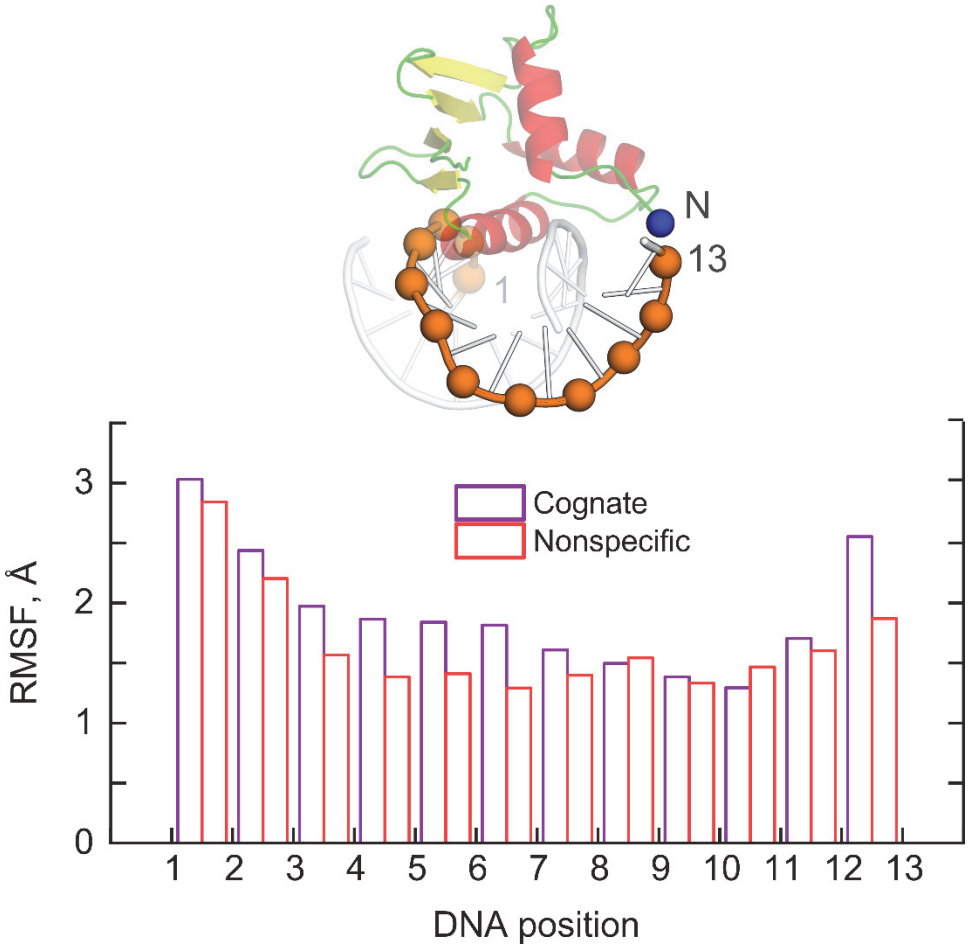

Figure S7. Backbone phosphate dynamics in Elk1-bound DNA. RMS fluctuations of the two anionic O atoms are shown at each position of the indicated DNA strand in the cognate and nonspecific Elk1 complex. Results from the final 200 μs of a representative 600 μs simulation are shown. The N-terminal cationic N atom is rendered as a blue sphere. The 13-bp DNA duplex was constructed with terminal hydroxyls. The numbered positions correspond to the position of the deoxyribose sandwiching the 12 phosphates, which are rendered as spheres in the averaged nonspecific structure shown. The phosphate O atoms at positions 1 and 13 are therefore internal atoms in the chain and separated from the fraying positions occupied by the terminal base pairs.

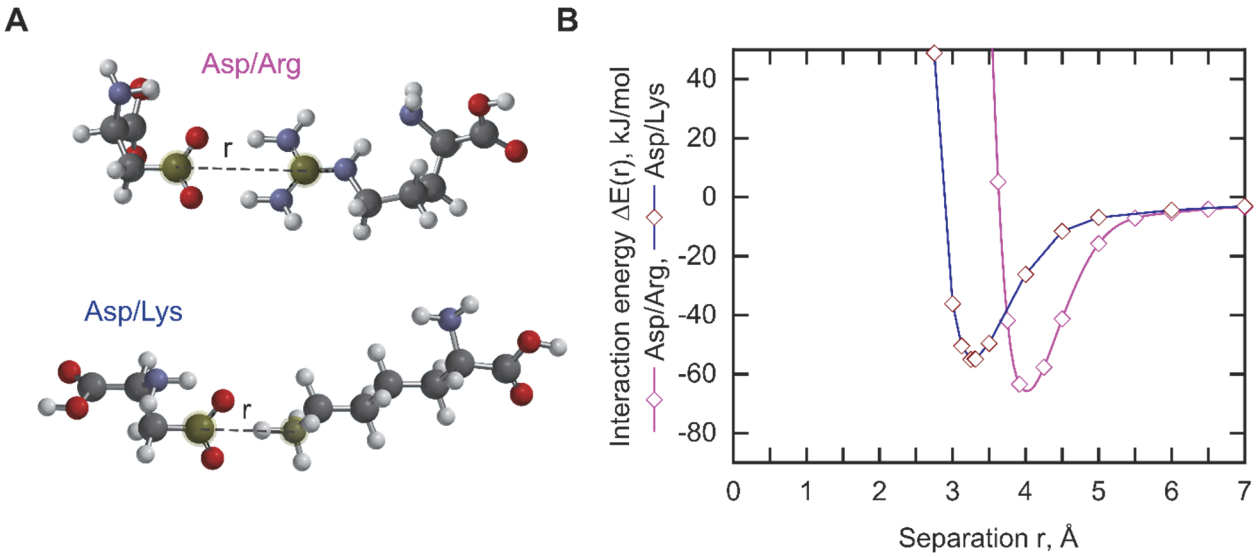

Figure S8. Interaction energies of Asp/Arg and Asp/Lys sidechains. A, Models of nonbonded Asp/Arg and Asp/Lys pairs following hybrid DFT geometry optimization at the ωB97x-D/6-31+G* level. **B**, Interaction energies of the nonbonded pairs as a function of separation distance r as indicated in Panel A. Single-point energies were evaluated with the 6-311++(2d,p) basis set, and referenced to 0 at r = 10 nm.